Adaptive velocity control of an autonomous vehicle using input-error model reference approach

Razminia, Abolhassan; Simorgh, Abolfazl; Marashian, Arash

Published in:
Journal of The Franklin Institute

DOI:
10.1016/j.jfranklin.2024.106700

Published: 06/04/2024

Document Version
Final published version

Journal of the Franklin Institute 361 (2024) 106700

Contents lists available at ScienceDirect

Journal of the Franklin Institute

journal homepage: www.elsevier.com/locate/fi

Adaptive velocity control of an autonomous vehicle using input-error model reference approach

Abolfazl Simorgh [a], Abolhassan Razminia [b,*], Arash Marashian [b]

[a] Department of Bioengineering and Aerospace Engineering, Universidad Carlos III de Madrid, Avenida de la Universidad, 30, Leganes, 28911 Madrid, Spain

[b] Process Control Laboratory, Faculty of Natural Sciences and Engineering, Åbo Akademi University, Turku, Finland

ARTICLE INFO

Keywords:
Velocity control
Model reference adaptive control
Input error
Robustness analysis
Higher-order tracking

ABSTRACT

The input error model reference adaptive control (IE-MRAC) is employed to regulate the longitudinal velocity of an autonomous vehicle to desired values by controlling both the throttle and the braking system. The proposed method deals with matching the unknown longitudinal model of the vehicle with a predefined model in the presence of various disturbances, including road conditions and aerodynamic effects. Moreover, it is shown that the saturation on the throttle and the brake pedals are successfully handled due to the properties of the derived error equation. Besides analyzing the natural properties of IE-MRAC, a novel stability proof of the closed-loop system is presented, and a robust modification of the adaptive control law is given as well. By using the proposed control technique, higher-order tracking is captured, and the effects on enhancing the vehicle responses are investigated. The applicability of the presented theoretical results is validated via the CarSim simulator.

1. Introduction

The 100-year-old servomechanism cruise control (CC) systems were designed to speed up the vehicle to achieve the desired speed that has been set by the driver [1]. Since the control actuator is only a throttle, the CC systems are applicable for speeds over 40 km/hr [1,2]. As has been proven in practice and studied enormously in the literature, the CC mechanism is unsuitable for controlling autonomous cars in urban traffic speeds because braking and accelerating systems are needed. An alternative solution is adaptive cruise control (ACC), in which the ability to brake in traffic situations is provided, and the velocity of vehicles can be controlled in the full range [1–5].

The perfect design of ACC systems plays a significant role in driving safety, fuel consumption, and the capacity of traffic [6,7]. The conventional ACC is designed in two parts, known as upper and lower-level control structures [2,8]. In the upper level, the desired velocity or acceleration is determined. In contrast, the lower level applies the brake/throttle signal command such that the specified acceleration or velocity from the upper level is followed. In the realm of ACC, a multitude of methods have been explored, including sliding mode control [9,10], control Lyapunov functions [11], adaptive control [3,8,12], fuzzy control [13,14], PID control [3,15], and model predictive control [15–17]. Each of these methods has proven effective in certain scenarios, with specific strengths and adaptability. However, the quest for a generic, adaptable, and robust control strategy remains challenging. This challenge arises from the diverse range of operational conditions, vehicle dynamics, and environmental factors a controller must manage effectively.

* Corresponding author.
E-mail addresses: abolfazl.simorgh@uc3m.es (A. Simorgh), abolhassan.razminia@abo.fi, razminia@pgu.ac.ir (A. Razminia), seyedarash.marashian@abo.fi (A. Marashian).

https://doi.org/10.1016/j.jfranklin.2024.106700
Received 24 June 2023; Received in revised form 11 January 2024; Accepted 21 February 2024
Available online 29 February 2024

For instance, in the case of the controller design proposed in [3], a system identification step is used first to determine the parameters of the considered model as a function of operating conditions, which are then used to generate control input. The controller's performance is heavily dependent on the accuracy of these estimated parameters. Achieving high accuracy in parameter estimation often requires persistent excitation, which is challenging to implement practically. For example, the authors in [3] noted the impracticality of using a pseudorandom binary sequence (PRBS) signal for the brake system, as it would cause frequent stopping. Furthermore, since the controller's efficacy is tightly coupled with the identified parameters, any change in vehicle or conditions (like environment, road surface, vehicle mass, etc.) might necessitate a complete re-identification process. The issues above persist with all adaptive and learning-based controller designs relying on exact system identification. Sliding mode control as a powerful, robust control strategy suffers from chattering, a phenomenon of high-frequency oscillations caused by the switching nature of the control law, leading to increased wear and tear on mechanical components [10]. Additionally, the implementation of SMC can be complex, especially in designing the sliding surface and ensuring system stability, and it may be sensitive to noise, which can amplify near the sliding surface and affect performance. The model predictive control, while offering optimal control solutions, heavily relies on the system model's accuracy, and inaccuracies can lead to suboptimal control [15]. PID Control, a widely used method, is most effective in linear systems and can struggle in systems with significant nonlinearities or varying dynamics. Tuning PID parameters to find the optimal balance can be a complex process, especially in systems with changing operating conditions. PID controllers also lack automatic adaptability to changes in system dynamics or external disturbances, often necessitating manual retuning [3]. The aforementioned challenges regarding complexity in controller design (e.g., SMC controller design), practical issues (e.g., the requirement for persistent excitation and chattering), case-dependency (e.g., exact model requirement, and need for retuning under varying operation conditions) motivated us introducing an approach facilitating an easy-to-use, flexible, and efficient control design for the ACC system under both internal and external uncertainty effects. The aim is to propose a generic control strategy that can be applied to a vast majority of vehicles without knowing the exact vehicle powertrain and brake system under different environmental conditions.

A robust adaptive controller for the lower-level structure of the ACC system is proposed in this study using the concept of model reference adaptive control. The model reference adaptive control serves as a control strategy to achieve the desired performance by dynamically adjusting the controller parameters based on the difference between the actual system's output and the desired reference model's output [18]. The goal is to make the actual system behave similarly to the reference model, even in the presence of uncertainties or changes in the system dynamics. This approach is particularly effective for ACC as the highly complex longitudinal model of an autonomous vehicle can be approximated with a simplified model and compelled to track a desired reference speed by real-time adjustments of the control parameters based on the observed behavior, allowing to adapt to changes in the system dynamics or operating conditions [19]. In this study, the direct MRAC is considered, avoiding the explicit necessity for accurate system identification before controller design, which can be practically challenging due to persistent excitation requirements. Therefore, the controller adapts directly to the observed system behavior without relying on a detailed model. The classical MRAC is based on the output error (OE-MRAC) [19,20]. Despite the simplicity in design, it suffers from different aspects, including the inability to handle the saturation on control signals (e.g., limits on the throttle) and the necessity of being strictly positive realness (SPR) of the reference model, which makes it unsuitable for the ACC system. To deal with these mentioned limitations, we propose the control design for the longitudinal velocity (LV) of autonomous vehicles based on the input-error MRAC (IE-MRAC) [18,21]. In addition to the mentioned drawbacks of the OE-MRAC, controller design based on IE-MRAC enables faster adaptation, improved tracking performance, reduced sensitivity to measurement noise, more suitable for non-minimum phase systems, easier adaptation in nonlinear systems, and more robust performance [22].

Our main contributions are given as follows:

(i) Designing an adaptive controller to regulate the speed of a vehicle by considering the throttle/brake mechanism as the control inputs and switching criterion between them.
(ii) Presenting a novel stability proof for the IE-MRAC and modifying it with a robust adaptive control law to guarantee the boundedness of controller parameters in the presence of uncertainties and disturbances.
(iii) Stating and proving the higher-order tracking (HOT) property of IE-MRAC for the first time in the literature. In the context of ACC, we show that by smoothing the reference command (i.e., desired velocity), second-order tracking will be achieved, leading to passenger comfort and reducing aging and maintenance costs.
(iv) Validating the proposed approach through its application to various classes of vehicles using the CarSim simulator. This validation was conducted under a range of challenging path conditions, encompassing road curves, banking, elevation changes, and aerodynamic effects, to ensure its effectiveness and robustness in diverse driving scenarios.

The manuscript is arranged as follows. Some preliminary backgrounds are reviewed in Section 2. Section 3 discusses the paper's main results: an adaptive control technique is developed whose stability is analyzed with some natural extensions. The numerical simulations are performed using CarSim to illustrate the obtained results in Section 4. Finally, several concluding remarks end the paper in Section 5.

Notation: A system with the transfer operator $\mathcal{G}(p)$, the input $u(t)$ and the output $y(t)$ is represented as $y(t) = \mathcal{G}(p)\{u(t)\}$ in which $p = \frac{\mathrm{d}}{\mathrm{d}t}$ is the differential operator; $\|\cdot\|$ denotes the Euclidean norm; $\mathscr{L}$ represents the Laplace operator.

Abbreviations: Model reference adaptive control (MRAC); Longitudinal velocity (LV); Longitudinal velocity control (LVC); Higher-order tracking (HOT); Input error MRAC (IE-MRAC); output error MRAC (OE-MRAC); Cruise control (CC).

2. Preliminaries

In this section, some preliminary facts are introduced so that the materials in the sequel can be simply followed.

2.1. Lemmas and Definitions

Definitions 1–3 and Lemmas 1, 2 are related to the rate of signals growth, which are needed for analyzing the boundedness of signals.

Definition 1 ([23]). Let $\alpha(\cdot)$, $\beta(\cdot) \in L_{\infty}^{e}$, where L_{∞}^{e} is the space of bounded functions for finite time:

(i) If there exists a continuous function $\upsilon(\cdot)$ such that $\lim_{t\to\infty} \upsilon(t) = 0$ and $\alpha(t) = \upsilon(t)\beta(t)$, then we define $\alpha(t) = \mathfrak{o}[\beta(t)]$.
(ii) If there exist constants k_1 and k_2 such that $\left|\alpha(t)\right| \le k_1 \left|\beta(t)\right| + k_2$, then we define $\alpha(t) = \mathfrak{O}[\beta(t)]$.

Definition 2 ([19]). Let $\alpha(\cdot)$, $\beta(\cdot) \in L_{\infty}^{e}$. If $\alpha(t) = \mathfrak{O}[\beta(t)]$ and $\beta(t) = \mathfrak{O}[\alpha(t)]$, then they are defined to be equivalent signals and signified as follows

$$\alpha(t) \equiv \beta(t).$$

Definition 3 ([19]). Let $\alpha(\cdot)$, $\beta(\cdot) \in L_{\infty}^{e}$. If $\sup_{\xi\le t}\left|\alpha(\xi)\right| \equiv \sup_{\xi\le t}\left|\beta(\xi)\right|$, then they are said to rise at the same rate.

Lemma 1 ([23]). *Let $\alpha(\cdot)$, $\beta(\cdot) \in L_{\infty}^{e}$, then we have*

$$\alpha(t) = \mathfrak{O}\left[\,\beta(t)\,\right] \quad \Leftrightarrow \quad \sup_{\xi\le t}\left|\alpha(\zeta)\right| = \mathfrak{O}\left[\,\beta(t)\,\right].$$

Lemma 2 ([24]). *Let $\alpha(t) = \Delta(s)\{\beta(t)\}$, where $\beta(\cdot) \in L_{\infty}^{e}$.*

(i) If $\Delta(s)$ be a strictly proper and stable filter, then $\left|\alpha(t)\right| = \mathfrak{O}\left[\,\sup_{\xi\le t}\left|\beta(\zeta)\right|\,\right]$.
(ii) If $\Delta(s)$ is a proper transfer function with Hurwitz numerator and denominator, then $\alpha(\cdot)$ and $\beta(\cdot)$ grow at the same rate.

In analyzing the HOT, the following definition is stated as a necessary and sufficient condition to prove signals converging to zero.

Definition 4. For a signal $z(t)$ defined on $[0,\infty)$, if for every $S > 0$, there exists a $\mathcal{T} = \mathcal{T}(S) > 0$ so that $\left|z(t)\right| < 0$ for all $t > \mathcal{T}$, then $z(t)$ vanishes asymptotically to zero.

2.2. Direct model reference adaptive control

In the following, the commonly employed MRAC approach, called output-error-based MRAC, is briefly presented, and its limitations in the context of ACC systems are discussed.

The objective of the MRAC is to seek a control law ($u(t)$) that causes the output of an unknown system:

$$\upsilon(t) = \mathcal{P}(s)\{u(t)\}, \quad \mathcal{P}(s) = \gamma\frac{n_p(s)}{p_p(s)} \tag{1}$$

to follow the output of a reference model:

$$\upsilon_m(t) = \mathcal{M}(s)\{r(t)\}, \quad \mathcal{M}(s) = \gamma_m\frac{n_m(s)}{p_m(s)} \tag{2}$$

where υ is the output of the plant, $u(t)$ is the control input, $\mathcal{P}(s)$ is the transfer function of the plant, γ is the high-frequency gain, and $p_p(s)$ and $n_p(s)$ are monic polynomials of degree n and m, respectively. $\mathcal{M}(s)$ is the transfer function of the reference model, $\upsilon_m(t)$ is the output of the reference model, and $r(t)$ is the reference signal (i.e., desired velocity in our context). Similar to the assumption on the plant, $p_m(s)$ and $n_m(s)$ are considered as monic polynomials of degree n and m, respectively.

The general assumptions for deriving the OE-MRAC are as follows [18]:

$\mathcal{A}$-OE1. The plant is strictly proper and minimum phase
$\mathcal{A}$-OE2. The reference model is stable, minimum phase, and strictly positive real
$\mathcal{A}$-OE3. The relative degree of the reference model κ is equal to or larger than the relative degree of the plant η (though in the representation, we considered it equal).
$\mathcal{A}$-OE4. The reference command $r(t)$ is a bounded piecewise continuous signal
$\mathcal{A}$-OE5. γ is known.

According to the structure of the MRAC in literature [18,19], the throttle signal is considered to have the following form

$$u_t(t) = \frac{c}{\phi(s)}\{u(t)\} + \frac{d(s)}{\phi(s)}\{v(t)\} + c_0 r(t) \tag{3}$$

where $d(s)$ is a polynomial of $n-1$ one, c and c_0 are scalars and $\phi(s)$ is a monic Hurwitz polynomial $n-1$. As will be presented in Section 3, a second-order transfer function is considered for representing the longitudinal model of an autonomous vehicle. Therefore, we directly present the control strategy considering second-order systems (i.e., n=2). By substituting the controller Eq. (3) in Eq. (1), and equating the resulting transfer function (i.e., from $r(t)$ to $v(t)$) to the reference model Eq. (2), unique c_0^*, c^*, $d^*(s)$ exist such that the following equivalence is satisfied

$$\frac{c_0^* \gamma \tilde{p}_m \tilde{\phi}}{\gamma_m} = (\tilde{\phi} - c^*)\tilde{p}_p - \gamma \tilde{d}^* \tag{4}$$

where the tilde notation is used to represent a polynomial of s (e.g., $\tilde{p}_p := p_p(s)$). The equality Eq. (4) implies that the plant behaves similarly to the reference model by this choice of parameters. When the plant is known, c_0^*, c^*, $d^*(s)$ can be simply found, which refers to the model reference control. Dividing both sides of Eq. (4) by $\tilde{p}_p\tilde{\phi}$, and then applying the resulting transfer functions to the $u_t(t)$ signal, the following equation is achieved

$$c_0^* \tilde{\mathcal{M}}^{-1}\{v(t)\} = u_t(t) - \frac{c^*}{\tilde{\phi}}\{u_t(t)\} - \frac{\tilde{d}^*}{\tilde{\phi}}\{v(t)\} + \varepsilon(t)$$

where $\varepsilon(t)$ denotes the effect of initial conditions decaying exponentially in time and does not affect the properties of the adaptive structure [18]. Therefore, it is neglected for simplicity in the following derivations. Thus, the output can be written as follows

$$v(t) = \frac{1}{c_0^*}\tilde{\mathcal{M}}\{u_t(t) - \frac{c^*}{\tilde{\phi}}\{u_t(t)\} - \frac{\tilde{d}^*}{\tilde{\phi}}\{v(t)\}\}$$

and by defining the difference between the actual and model velocity as the output error, the following equation is achieved

$$e_o = v(t) - v_m(t) = \frac{1}{c_0^*}\tilde{\mathcal{M}}\{u_t(t) - \frac{c^*}{\tilde{\phi}}\{u_t(t)\} - \frac{\tilde{d}^*}{\tilde{\phi}}\{v(t)\} - c_0^* r(t)\}. \tag{5}$$

By defining the following vectors

$$\boldsymbol{\varphi} = \boldsymbol{\vartheta}(t) - \boldsymbol{\vartheta}^*, \quad \boldsymbol{\vartheta} = \begin{bmatrix} c_0 & c & d_0 & d_1 \end{bmatrix}^T, \quad \boldsymbol{\varpi} = \begin{bmatrix} r(t) & \varpi_1 & v(t) & \varpi_2 \end{bmatrix}^T \tag{6}$$

where $\boldsymbol{\varphi}$ denotes parameter errors and $\varpi_1 = \frac{1}{\tilde{\phi}(s)}\{u_t(t)\}$, $\varpi_2 = \frac{1}{\tilde{\phi}(s)}\{v(t)\}$ and

$$\frac{\tilde{d}}{\tilde{\phi}}\{v(t)\} = d_0 v(t) + \frac{d_1}{\tilde{\phi}(s)}\{v(t)\}$$

the output error is rewritten as the following equation

$$e_o = v(t) - v_m(t) = \frac{1}{c_0^*}\tilde{\mathcal{M}}\{\boldsymbol{\varphi}^T(t)\boldsymbol{\varpi}(t)\}. \tag{7}$$

leading to the following gradient algorithm for updating controller parameters:

$$\dot{\boldsymbol{\varphi}}(t) = \dot{\vartheta}(t) = -\boldsymbol{\Gamma} e_o(t)\boldsymbol{\varpi}(t) \tag{8}$$

where $\boldsymbol{\Gamma} \in \mathbb{R}^{4\times 4}$ is a diagonal matrix with positive arrays that regulates the rate of parameter convergence.

Remark 1. There exist specific limitations with applying OE-MRAC for the ACC system, listed in the following:

- The derived error equation given in Eq. (7) has the form of the well-known strictly positive real (SPR) error equation. To guarantee the stability of the adaptive control design using projection update law, the reference model $\tilde{\mathcal{M}}$ must be SPR. Satisfying such a strict condition may not be possible in some problems like the one considered in this manuscript (i.e., the relative degree of $\tilde{\mathcal{M}}$ is two) Several methods, such as defining an augmented error, have been suggested in the literature to cope with this issue [18,19].
- It is necessary to know the high-frequency gain (e.g., γ in this paper), or at least its sign.
- The derivation of the error equation assumes that the input signal $u_t(t)$ consistently equals the computed value $u_t(t) = \vartheta^T\boldsymbol{\varpi}$ at all times. However, should the input experience saturation (e.g., limits on the throttle), this could lead to erroneous updates of the identifier [18].

In the next section, we will propose the input-error-based direct MRAC design, addressing the limitations above of the OE-MRAC for the ACC system.

3. Control design

In this section, the essential achievements of the paper will be presented through four subsections. As a first step, a brief model description of the LV is given. Then, the IE-MRAC is designed to control the speed of an autonomous vehicle, which is provided in Section 3.1. The stability of the proposed controller design is developed in Section 3.2, and subsection 3.3 reveals some essential properties of the IE-MRAC method known as HOT. The controller design presented in Section 3.1 considers the idealized situations. Due to the presence of uncertainties, the controller is to be modified in order to ensure stability, presented in subsection 3.4.

3.1. Longitudinal dynamical model of an autonomous vehicle

According to Newton's second law, the balance of longitudinal forces on a car is obtained as the following relation [1]

$$\mathcal{M}_v \dot{v} = \sum_{i,j=1}^{2} \mathcal{F}_{x_{ij}} - \sum_{i,j=1}^{2} \mathcal{R}_{x_{ij}} - \mathcal{F}_a - \mathcal{F}_\theta \tag{9}$$

where $\mathcal{M}_v$ is the vehicle mass, v is the LV, $F_{x_{ij}}$ and $\mathcal{R}_{x_{ij}}$ are the longitudinal and rolling resistance forces acting on each wheel, respectively, $\mathcal{F}_a$ and $\mathcal{F}_\theta$ are the longitudinal aerodynamic drag and road inclination forces. In [1], Chapter 4 is fully devoted to details and modeling of these forces. Considering no-slip situations, $\mathcal{F}_{x_{ij}}$ for $i, j = 1, 2$ can be considered as the sum of the brake and the engine forces as

$$\sum_{i,j=1}^{2} \mathcal{F}_{x_{ij}} = \mathcal{F}_{eng} + \mathcal{F}_{bra}.$$

An idealized condition is considered initially for developing the longitudinal model of an autonomous vehicle, where the vehicle moves through a flat surface with no brake. Consequently, $\mathcal{F}_{eng}$ can be considered the dominant force controlling the movement. The engine force is shifted to the vehicle by the transmission system, which raises difficulty in modeling the longitudinal dynamic due to the presence of nonlinear behavior. Instead, we employ a simplified second-order model to capture the relation between throttle as control input and longitudinal velocity outputted from the high-fidelity simulator (i.e., CarSim) under specific operating conditions, verified through experiments (see [3]). Thus, the following input–output description with the unknown slowly time-varying parameters is assumed to represent the LV dynamics

$$v(t) = \mathcal{P}(s)\{u_t(t)\}, \quad \mathcal{P}(s) = \frac{\gamma}{s^2 + \beta_1 s + \beta_0} = \frac{\gamma}{p_p(s)} \tag{10}$$

where $\mathcal{P}(s)$ is the frequency domain representation of the LV dynamics with the unknown parameters β_1, β_0, and γ that refers to the system specifications around operating conditions. $v(t)$ is the LV, and $u_t(t)$ is the throttle level. As will be shown in the simulation results, a significant contribution of this paper lies in demonstrating that, despite the strictly linear nature of the selected model, we have the capability to adjust its parameters based on the vehicle's operating points. This approach effectively captures the nonlinear behaviors of the engine and the transmission. Such an approach has been verified in the earlier study [3]. In contrast to the approach in [3], which necessitates a system identification step followed by controller design based on the identified system parameters, our proposed method, as will be shown in the next section, involves direct adaptation of controller parameters. This adaptation is based on the received input/output and error signals, thereby diminishing the reliance on precise model identification and enhancing the generality of the approach.

3.2. Input-error MRAC design for ACC systems

In this section, we will propose input-error-based direct MRAC for the control design of the ACC system. We first define a second-order reference model as:

$$v_m(t) = \mathcal{M}(s)\{r(t)\}, \quad \mathcal{M}(s) = \frac{\gamma_m}{s^2 + 2\zeta w_n s + w_n^2} = \frac{\gamma_m}{p_m(s)}. \tag{11}$$

The assumptions that will be used for the IE-MRAC are listed as follows:

$\mathcal{A}$-IE1. The plant is strictly proper and minimum phase
$\mathcal{A}$-IE2. The reference model is a stable and minimum phase
$\mathcal{A}$-IE3. The relative degree of the reference model κ is equal to or larger than the relative degree of the plant η
$\mathcal{A}$-IE4. The reference command $r(t)$ is a bounded piecewise continuous signal
$\mathcal{A}$-IE5. The upper bound on the γ is known.

As can be understood from the assumptions, the SPR condition and the necessity to have complete information on γ (at least the sign) are no longer needed. Besides, as will be discussed throughout the paper and verified in the simulation results, the IE-MRAC demonstrates superior performance over OE-MRAC in several aspects. These include enhanced handling of saturation, improved robustness, and the feasibility of employing more effective adaptive laws, such as the normalized gradient algorithm, as highlighted in the works of [18,21].

Let us proceed with designing the IE-MRAC controller for the ACC system. We first divide both sides of Eq. (4) by $\tilde{p}_p \tilde{\phi} \tilde{\mathcal{L}}$, and then apply the resulting transfer functions to $u_t(t)$

$$\tilde{\mathcal{L}}^{-1}\{u_t(t)\} - c^*(\tilde{\mathcal{M}}\tilde{\mathcal{L}})^{-1}\{v(t)\} = \tilde{\mathcal{L}}^{-1}\frac{\tilde{d}^*}{\tilde{\phi}}\{v(t)\} + \tilde{\mathcal{L}}^{-1}\frac{\tilde{c}^*}{\tilde{\phi}}\{u_t(t)\} + \varepsilon(t) \tag{12}$$

where $\tilde{\mathcal{L}}^{-1}$ is a stable and minimum phase filter to be determined such that $(\tilde{\mathcal{L}}\tilde{\mathcal{M}})^{-1}$ is a proper transfer function, and $\varepsilon(t)$ shows the effect of initial conditions. By defining the following vectors

$$\begin{aligned} &\bar{\vartheta}^* = \begin{bmatrix} c^* & d_0^* & d_1^* \end{bmatrix}^T, \quad \bar{\varpi}(t) = \begin{bmatrix} \frac{1}{\tilde{\phi}}\{u_t(t)\} & v(t) & \frac{1}{\tilde{\phi}}\{v(t)\} \end{bmatrix}^T, \quad \Xi(t) = \tilde{\mathcal{L}}^{-1}\{\Sigma(t)\} \\ &\Sigma(t) = \begin{bmatrix} \tilde{\mathcal{M}}^{-1}\{v(t)\} & \bar{\varpi} \end{bmatrix}^T \end{aligned} \tag{13}$$

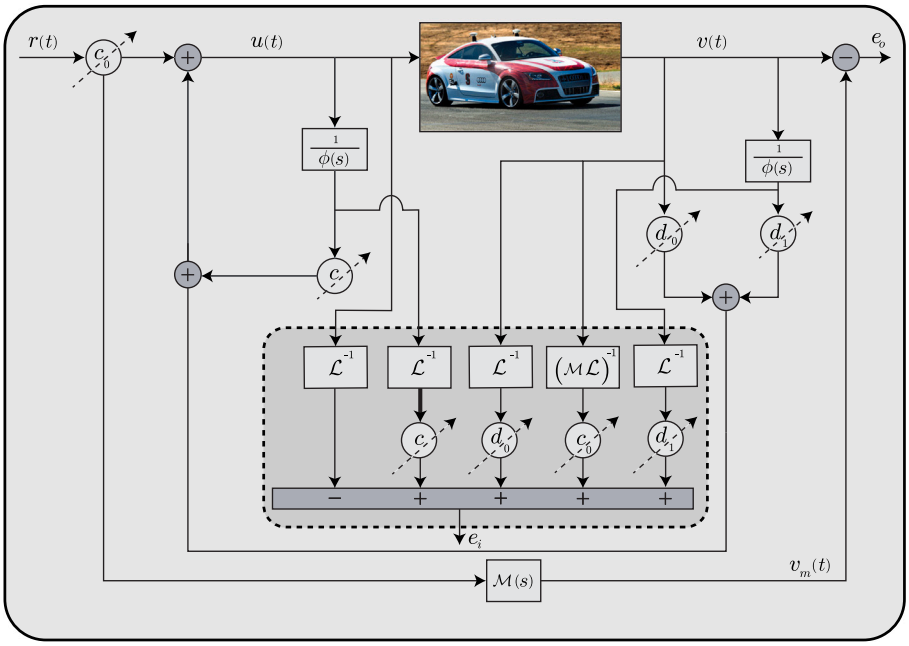

Fig. 1. Block diagram representation of IE-MRAC.

Eq. (12) can be written as the following equation

$$\tilde{\mathcal{L}}^{-1}\{u_t(t)\} = \boldsymbol{\vartheta}^{*T}\,\boldsymbol{\Xi}(t) + \varepsilon(t). \tag{14}$$

Now, the input error can be defined as follows

$$e_i = \boldsymbol{\vartheta}^T(t)\boldsymbol{\Xi}(t) - \tilde{\mathcal{L}}^{-1}\{u_t(t)\} = \boldsymbol{\varphi}^T(t)\boldsymbol{\Xi}(t) - \varepsilon(t) \tag{15}$$

which is the form of linear regression. As can be seen, the strict SPR assumption is avoided, and in addition to the projection update law, other well-known algorithms can be employed. Since the normalized gradient algorithm has good convergence properties, it is chosen to update the controller parameters in this paper

$$\dot{\boldsymbol{\varphi}}(t) = \dot{\boldsymbol{\vartheta}}(t) = -\boldsymbol{\Gamma}\frac{e_i\boldsymbol{\Xi}(t)}{1+\zeta\boldsymbol{\Xi}^T(t)\boldsymbol{\Xi}(t)} \tag{16}$$

where $\boldsymbol{\Gamma} \in \mathbb{R}^{4\times4}$ is a diagonal matrix with positive arrays that regulates the rate of parameter convergence, and ζ is a positive constant. The selection of these parameters is crucial and necessitates a careful balance between stability, speed of adaptation, responsiveness, and noise sensitivity. Large $\boldsymbol{\Gamma}$ generally leads to a quicker adaptive response, beneficial for rapidly changing dynamic systems and fast-tracking objectives. However, it may induce instability, particularly when the error gradient is substantial. Other drawbacks include oscillations and heightened sensitivity to noise. Large ζ effectively prevents instability caused by small values in the normalization factor, particularly when the error gradient is minimal. On the flip side, this can reduce the system's sensitivity to changes in the error gradient, resulting in slower adaptation rates. For this study, we take into account these trade-offs to optimize the performance of the adaptive control approach. Notice that the effects of the initial condition have been neglected in deriving the adaptive law in Eq. (16). In Appendix A, we show that neglecting this exponentially decaying term does not affect the stability analysis. The signal flow graph of the input error scheme is illustrated in Fig. 1.

4. Stability analysis

In the view of the normalized gradient algorithm Eq. (16), the boundedness of $\boldsymbol{\varphi}$ and its derivative $\dot{\boldsymbol{\varphi}}$ is resulted [18,23,25]. Moreover, it can be concluded that

$$\mu = \frac{e_i(t)}{\sqrt{1+\zeta\boldsymbol{\Xi}^T(t)\boldsymbol{\Xi}(t)}} \in L_2 \tag{17}$$

which in turn results in $\dot{\boldsymbol{\varphi}} \in L_2$ [19]. In addition to the boundedness of controller parameters, the boundedness of all signals is needed to show $\lim_{t\to\infty} e_i(t) = 0$ and, in turn, concluding the convergence of output error to zero (i.e., $\lim_{t\to\infty} e_o(t) = 0$). In this section, using the idea of the ordering of signals [23], a novel stability proof is developed for IE-MRAC. The stability proof is given for the LVC. However, it can be extended to a general case by following the same line in proving stability.

The steps for proving stability are as follows. First, a lemma is stated and proven that says if signals $\left|v(t)\right|$, $\left\|\boldsymbol{\varpi}(t)\right\|$, $\left\|\boldsymbol{\Xi}(t)\right\|$ and $\left\|\boldsymbol{\Sigma}(t)\right\|$ grow in an unbounded fashion, they grow at the same rate. In the next step, by analyzing the input and output errors, it is shown that the same signals grow at different rates, which contradicts the former assumption. Therefore, by showing such a contradiction, the boundedness of all signals can be concluded, which results in

$$\lim_{t\to\infty} e_i(t) = 0.$$

Before continuation, a necessary lemma is presented.

Lemma 3. *Let* $\boldsymbol{\Gamma}^T := \begin{bmatrix}\boldsymbol{\Gamma}_1^T & \boldsymbol{\Gamma}_2^T & \cdots & \boldsymbol{\Gamma}_n^T\end{bmatrix}$ *where* $\boldsymbol{\Gamma} : \mathbb{R}^+ \to \mathbb{R}^n$, $\boldsymbol{\Gamma}_i : \mathbb{R}^+ \to \mathbb{R}^{n_i}$ *for* $i = 1, \dots, n$ *and* $n_i \in \mathbb{N}$ *such that* $\sum_{i=1}^n n_i = n$. *If* $\boldsymbol{\Gamma}$ *rises in unbounded fashion, then*

$$\sup_{\substack{\xi\le t\\ 1\le i\neq j\le n}} \left\|\boldsymbol{\Gamma}_i(\xi)\right\| = \mathfrak{O}\left[\sup_{\xi\le t}\left\|\boldsymbol{\Gamma}_j(\xi)\right\|\right] \quad \textit{if and only if} \quad \sup_{\xi\le t}\left\|\boldsymbol{\Gamma}_j(\xi)\right\| \equiv \sup_{\xi\le t}\left\|\boldsymbol{\Gamma}(\xi)\right\|. \tag{18}$$

Proof. Since $\left\|\boldsymbol{\Gamma}\right\|^2 = \sum_{i=1}^n \left\|\boldsymbol{\Gamma}_i\right\|^2$, one can conclude

$$\sup_{\xi\le t}\left\|\boldsymbol{\Gamma}(\xi)\right\|^2 - \sum_{k=1\neq i}^{n}\sup_{\xi\le t}\left\|\boldsymbol{\Gamma}_k(\xi)\right\|^2 \le \kappa_i^2 \sup_{\xi\le t}\left\|\boldsymbol{\Gamma}_j(\xi)\right\|^2, \qquad \forall i : 1 \le i \neq j \le n. \tag{19}$$

from Lemma 1. Repeating this inequality Eq. (19) for all i's, we can finally conclude

$$(n-1)\sup_{\xi\le t}\left\|\boldsymbol{\Gamma}(\xi)\right\|^2 \le \Big(\sum_{i=1\neq j}^{n}\kappa_i^2 + 1\Big)\sup_{\xi\le t}\left\|\boldsymbol{\Gamma}_j(\xi)\right\|^2 + (n-2)\sup_{\xi\le t}\left\|\boldsymbol{\Gamma}(\xi)\right\|^2$$

$$\sup_{\xi\le t}\left\|\boldsymbol{\Gamma}(\xi)\right\|^2 \le \bar{\kappa}^2 \sup_{\xi\le t}\left\|\boldsymbol{\Gamma}_j(\xi)\right\|^2$$

where $\bar{\kappa}^2 = (\sum_{i=1\neq j}^n \kappa_i^2 + 1)$, which in turn results in

$$\sup_{\xi\le t}\left\|\boldsymbol{\Gamma}(\xi)\right\| = \mathfrak{O}\left[\sup_{\xi\le t}\left\|\boldsymbol{\Gamma}_j(\xi)\right\|\right].$$

Since $\left\|\boldsymbol{\Gamma}(t)\right\| = \mathfrak{O}\left[\sup_{\xi\le t}\left\|\boldsymbol{\Gamma}(\xi)\right\|\right]$, $\sup_{\xi\le t}\left\|\boldsymbol{\Gamma}_j(\xi)\right\| = \mathfrak{O}\left[\sup_{\xi\le t}\left\|\boldsymbol{\Gamma}(\xi)\right\|\right]$ can be directly resulted. Thus

$$\sup_{\xi\le t}\left\|\boldsymbol{\Gamma}_j(\xi)\right\| \equiv \sup_{\xi\le t}\left\|\boldsymbol{\Gamma}(\xi)\right\|$$

which proves the sufficiency part. To prove the necessity, we can utilize a similar approach. □

Now, the central lemma in proving the boundedness of signals is stated.

Lemma 4. *Consider the IE-MRAC structure; if the signals in the adaptive loop rise in an unbounded sense,* $\left|v(t)\right|$, $\left\|\boldsymbol{\varpi}(t)\right\|$, $\left\|\boldsymbol{\Xi}(t)\right\|$ *and* $\left\|\boldsymbol{\Sigma}(t)\right\|$ *rise at the same rate.*

Proof. Since the parameter error vector is uniformly bounded, all signals in the adaptive loop can grow at most exponentially and, therefore, belong to L_∞^e. As $v(\cdot)$ is related to $\varpi(\cdot)$ through a linear exponentially stable filter Eq. (6), one can result

$$\left|\boldsymbol{\varpi}_2(t)\right| = \mathfrak{O}\left[\sup_{\xi\le t}\left|v(\xi)\right|\right]. \tag{20}$$

from Lemma 2. Considering the update law Eq. (16), $\boldsymbol{\vartheta}(t)$ is bounded, thus $\boldsymbol{\varpi}(t)$ can rise at most exponentially. The reason is that $\boldsymbol{\varpi}(t)$ is the state of the LTV system with bounded parameters Eq. (39). Therefore, the following inequality is held

$$\left|\dot{\varpi}_1(t)\right| \le \kappa_1\left\|\boldsymbol{\varpi}(t)\right\| + \kappa_2$$

where $\kappa_1, \kappa_2 \in \mathbb{R}^+$. As $\tilde{\mathcal{P}}\{\boldsymbol{\varpi}_1\} = \boldsymbol{\varpi}_2$, and $\tilde{\mathcal{P}}$ has Hurwitz numerator, according to the Corollary 4 in [23], we can write

$$\left|\boldsymbol{\varpi}_1(t)\right| = \mathfrak{O}\left[\sup_{\xi\le t}\left|\boldsymbol{\varpi}_2(\xi)\right|\right]. \tag{21}$$

By using Lemma 3 and Eqs. ((20),(21)) we can say that $v(t)$ and $\boldsymbol{\varpi}(t)$ grow at the same rate

$$\sup_{\xi\le t}\left\|v(\xi)\right\| \equiv \sup_{\xi\le t}\left\|\boldsymbol{\varpi}(\xi)\right\|. \tag{22}$$

As can be concluded from Lemma 2, $(\tilde{\mathcal{M}}\tilde{\mathcal{L}})^{-1}\{v(t)\}$ and $v(t)$ grow at the same rate, moreover, Lemma 2 implies that

$$\left|\tilde{\mathcal{L}}^{-1}\{\varpi_1(t)\}\right| = \mathfrak{O}\left[\sup_{\xi\le t}\left|\varpi_1(\xi)\right|\right] = \mathfrak{O}\left[\sup_{\xi\le t}\left|v(\xi)\right|\right]$$

$$\left|\tilde{\mathcal{L}}^{-1}\{\varpi_2(t)\}\right| = \mathfrak{O}\left[\sup_{\xi\le t}\left|\varpi_2(\xi)\right|\right] = \mathfrak{O}\left[\sup_{\xi\le t}\left|v(\xi)\right|\right]$$

$$\left|\tilde{\mathcal{L}}^{-1}\{v(t)\}\right| = \mathfrak{O}\left[\sup_{\xi\le t}\left|v(\xi)\right|\right]$$

which in turn results in

$$\sup_{\xi\le t}\left|v(\xi)\right| \equiv \sup_{\xi\le t}\left\|\Xi(\xi)\right\|$$

that shows $v(t)$ and $\Xi(t)$ rise at the same rate. By defining $r_s(t) := \tilde{\mathcal{M}}^{-1}\{v(t)\}$ and applying $\tilde{\mathcal{L}}$ to the both sides of Eq. (12), we have

$$u_t(t) = c_0^* r_s(t) + \bar{\vartheta}^{*^T}\bar{\varpi}(t)$$

which is equal to $u_t(t) = \vartheta^T(t)\varpi(t)$ Eq. (3). By some algebraic manipulation, $r_s(t)$ can be written as the following equation

$$r_s(t) = r(t) + \frac{1}{c_0^*}\boldsymbol{\varphi}^T(t)\boldsymbol{\varpi}(t).$$

Since $\boldsymbol{\varphi}$ is uniformly bounded, the following relation can be concluded (see Lemma 3 in [23])

$$\left|r_s(t)\right| = \mathfrak{O}\left[\sup_{\xi\le t}\left\|\boldsymbol{\varpi}(\xi)\right\|\right]$$

which in turn results in $\left|r_s(t)\right| = \mathfrak{O}\left[\sup_{\xi\le t}\left|v(\xi)\right|\right]$ by using Eq. (22). Consequently, by employing Lemma 3, it can be shown that $v(t)$ and $\boldsymbol{\Sigma}(t)$ grow at the same rate, which completes the proof. □

Theorem 1. *Let us consider a second-order system ($\mathcal{P}(s)$) representing the longitudinal dynamics of an autonomous vehicle with unknown slowly varying parameters given in Eq. (10), a second-order reference model ($\mathcal{M}(s)$) given in Eq. (2), and a bounded (piecewise) continuous signal $r(t)$, satisfying assumptions A-IE1-A-IE5. The control law $u_t(t) = \vartheta^T\varpi$ with the following identifier structure*

$$\begin{aligned}\Xi(t) &= \tilde{\mathcal{L}}^{-1}\left\{\left[\tilde{\mathcal{M}}^{-1}\{v(t)\} \quad \tfrac{1}{\tilde{\phi}}\{u_t(t)\} \quad v(t) \quad \tfrac{1}{\tilde{\phi}}\{v(t)\}\right]^T\right\}\\ e_i(t) &= \vartheta^T(t)\Xi(t) - \tilde{\mathcal{L}}^{-1}\{u_t(t)\}\end{aligned} \tag{23}$$

and the normalized gradient algorithm to update controller parameters

$$\dot{\boldsymbol{\varphi}}(t) = \dot{\vartheta}(t) = -\boldsymbol{\Gamma}\frac{e_i\Xi(t)}{1+\zeta\Xi^T(t)\Xi(t)} \tag{24}$$

guarantees the boundedness of all states within the adaptive system, and the velocity of the autonomous vehicle tracks the output of the reference model as t approaches infinity, i.e., $\lim_{t\to\infty} e_o(t) = \lim_{t\to\infty} v(t) - v_m(t) = 0$. In Eq. (23), $\phi(s)$ is a monic Hurwitz polynomial of degree 1 and $\mathcal{L}^{-1}(s)$ is a stable and minimum phase filter to be determined such that $(\mathcal{L}(s)\mathcal{M}(s))^{-1}$ is a proper transfer function.

Proof. It was shown in Lemma 4 that if signals grow unboundedly, they grow at the same rate. We start by assuming all the signals in the adaptive system grow in an unbounded manner. By using Swapping Lemma [18], one can write the relation between the output and input error as follows

$$e_0(t) = v(t) - v_m(t) = \tilde{\mathcal{M}}\tilde{\mathcal{L}}\{\frac{1}{c_0(t)}\boldsymbol{\varphi}^T(t)\Xi(t)\} + \tilde{\mathcal{M}}\tilde{\mathcal{L}}\tilde{\mathcal{K}}_c^{-1}\{\tilde{\mathcal{K}}_b^{-1}\{\boldsymbol{\Sigma}^T\}\{\frac{\dot{\varphi}}{c_0}\}\} \tag{25}$$

where here $\tilde{\mathcal{L}}^{-1}$ is used instead of $\tilde{\mathcal{L}}$ in the swapping Lemma. Considering the properties of the normalized gradient algorithm, we can establish (Eq. (17))

$$\boldsymbol{\varphi}^T(t)\Xi(t) = \mu\cdot\sqrt{1+\zeta\Xi^T(t)\Xi(t)}$$

where $\mu\in L_2$. Because it is assumed that the upper bound on $\gamma\le\gamma_{max}$ is known ($\mathcal{A}$-IE5) (i.e., lower bound on c_0 is known), $c_0^{-1}(t)$ is bounded, which implies

$$\begin{aligned}\tilde{\mathcal{M}}\tilde{\mathcal{L}}\{\frac{1}{c_0(t)}\boldsymbol{\varphi}^T(t)\Xi(t)\} &= \mathfrak{o}\left[\sup_{\xi\le t}\left\|\Xi(\zeta)\right\|\right]\\ \tilde{\mathcal{M}}\tilde{\mathcal{L}}\tilde{\mathcal{K}}_c^{-1}\{\tilde{\mathcal{K}}_b^{-1}\{\boldsymbol{\Sigma}^T\}\{\frac{\dot{\varphi}}{c_0}\}\} &= \mathfrak{o}\left[\sup_{\xi\le t}\left\|\boldsymbol{\Sigma}(\zeta)\right\|\right]\end{aligned}$$

from Lemma 2.9 in [19]. Since $\Xi(t)$ and $\boldsymbol{\Sigma}(t)$ grow at the same rate, we can write

$$\left|v(t)\right| = \mathfrak{o}\left[\sup_{\xi\le t}\left\|\boldsymbol{\Sigma}(\xi)\right\|\right]$$

which contradicts the statement of growing at the same rate, and as a result, all signals are uniformly bounded.

In the next step, the convergence of $e_i(t)$ and $\dot{\phi}$ to zero is proven. Based on the used normalized gradient update law, we have $\dot{\boldsymbol{\varphi}}\in L_2\bigcap L_\infty$. From $\dot{\boldsymbol{\varphi}}\in L_2$, $e_i(t)\in L_2$ is concluded. In order to show the convergence of $\lim_{t\to\infty} e_i(t) = 0$ and also $\lim_{t\to\infty}\dot{\varphi}_i(t) = 0$, $\dot{e}_i(t) = \dot{\boldsymbol{\varphi}}^T(t)\Xi(t) + \boldsymbol{\varphi}^T(t)\dot{\Xi}(t)$ needs to bounded. For the boundedness of $\dot{e}_i(t)$, we need to show the boundedness of $\boldsymbol{\varphi}^T(t)\dot{\Xi}(t)$. The Eq. (13) implies that the boundedness of $\dot{v}(t)$ is needed for showing the boundedness of $\boldsymbol{\varphi}^T(t)\dot{\Xi}(t)$. By taking the first-order derivative from Eq. (7), the following equation is obtained

$$\dot{v}(t) = \dot{v}_m(t) + \frac{1}{c_0^*}\tilde{\mathcal{M}}s\{\boldsymbol{\varphi}^T(t)\boldsymbol{\varpi}(t)\} = \tilde{\mathcal{M}}s\{r(t) + \frac{1}{c_0^*}\varphi^T(t)\boldsymbol{\varpi}(t)\} \tag{26}$$

where $\dot{v}(t)$ is related to the bounded signal $r(t)+\frac{1}{c_0^*}\varphi^T(t)\varpi(t)$ through the strictly proper and stable transfer function $\tilde{\mathcal{M}}s$, thus, it is bounded. Therefore, $e_i(t)\in L_2\bigcap L_\infty$, and $\dot{e}_i(t)\in L_\infty$. Using Barbalat's lemma, the convergence of $e_i(t)$ and, therefore, $\dot{\phi}$ to zero is guaranteed.

To ensure the convergence of the output error to zero, we need to show that the right-hand side of Eq. (25) tends to zero for sufficiently large t. By defining

$$z_1(t)=\tilde{\mathcal{M}}\tilde{\mathcal{L}}\{\frac{1}{c_0}\boldsymbol{\varphi}^T(t)\boldsymbol{v}(t)\} \tag{27}$$

$$z_2(t)=\tilde{\mathcal{M}}\tilde{\mathcal{L}}\tilde{\mathcal{K}}_c^{-1}\{\tilde{\mathcal{K}}_b^{-1}\{\Xi^T\}\{\frac{\dot{\varphi}}{c_0}\}\} \tag{28}$$

the objective is to ensure the convergence of the following equation to zero

$$\lim_{t\to\infty}e_o(t)=\lim_{t\to\infty}z_1(t)+\lim_{t\to\infty}z_2(t)=0.$$

As a first step, the following filters are defined

$$\lambda(s)=\frac{\varrho^2}{s^2+2\varrho s+\varrho^2},\quad s\Pi(s)=1-\lambda(s)=\frac{s^2+2\varrho s}{s^2+2\varrho s+\varrho^2} \tag{29}$$

where ϱ is a constant parameter to be determined. As can be seen from Eq. (29), $\Pi(s)$ is a stable and strictly proper which has the following L_1 norm

$$\left\|\pi(t)\right\|_1=\left\|\mathscr{L}^{-1}\{\Pi(s)\}\right\|_1=\frac{2}{\varrho} \tag{30}$$

where $\mathscr{L}^{-1}\{\cdot\}$ is the Laplace inverse operator. Applying both sides of Eq. (27) by $s\Pi(s)+\lambda(s)=1$, the following equation is received

$$z_1(t)=\underbrace{\tilde{\Pi}\tilde{\mathcal{M}}\tilde{\mathcal{L}}s\{\frac{1}{c_0(t)}\boldsymbol{\varphi}^T(t)\Xi(t)\}}_{z_{11}(t)}+\underbrace{\tilde{\lambda}\tilde{\mathcal{M}}\tilde{\mathcal{L}}\{\frac{1}{c_0(t)}\boldsymbol{\varphi}^T(t)\Xi(t)\}}_{z_{12}(t)}. \tag{31}$$

As $\tilde{\lambda}\tilde{\mathcal{M}}\tilde{\mathcal{L}}$ is a stable and strictly proper transfer function, $c_0^{-1}(t)$ is bounded by assumption, and $\lim_{t\to\infty}e_i(t)=0$, it can be concluded that the second term of Eq. (31) converges to zero for sufficiently large t. To analyze the first term of Eq. (31), the boundedness of $s\{c_0^{-1}(t)\boldsymbol{\varphi}^T(t)\Xi(t)\}$ is considered, which can be written as

$$s\{\frac{1}{c_0(t)}\boldsymbol{\varphi}^T(t)\Xi(t)\}=\frac{c_0(t)[\dot{\boldsymbol{\varphi}}^T(t)\Xi(t)+\boldsymbol{\varphi}^T(t)\dot{\Xi}(t)]-\boldsymbol{\varphi}^T(t)\Xi(t)\dot{c}_0(t)}{c_0^2(t)} \tag{32}$$

where the boundedness of terms can be simplicity verified (see properties of update laws Eq. (16)). Since Eq. (32) is bounded and $\tilde{\mathcal{M}}\tilde{\mathcal{L}}$ is stable and proper, using $z_{11}(t)$ and the well-known norm inequality, it can be concluded that

$$\left|z_{11}(t)\right|\le\left\|\pi(t)\right\|_1=\frac{\beta}{\varrho} \tag{33}$$

for some constant β independent of $\varrho>0$. To show the convergence of $z_1(t)$, the approach of [26] is employed. According to Definition 4, we need to show that there is a $\mathcal{T}>0$, for every $S>0$ so that $\left|z_1(t)\right|<S$ for all $t>\mathcal{T}$. By choosing $\varrho=2\beta S^{-1}$ in Eq. (29) such that $\beta\varrho^{-1}\le 0.5S$ in Eq. (33), and assuming $\mathcal{T}=\mathcal{T}_\varrho(\varrho(S),S):=\mathcal{T}(S)>0$, such that $\left|z_{12}(t)\right|<0.5S$ for all $t>\mathcal{T}$, we have

$$\left|z_1(t)\right|\le\left|z_{11}(t)\right|+\left|z_{12}(t)\right|<0.5S+0.5S=S \tag{34}$$

for all $t>\mathcal{T}$. By referring to Definition 4, Eq. (34) implies $\lim_{t\to\infty}z_1(t)=0$. Notice that, $\left|z_{12}(t)\right|<0.5S$ for all $\mathcal{T}(S)>0$ is guaranteed owing to the property of the convergence of $z_{12}(t)$ to zero.

Since $c_0^{-1}(t)$ is bounded, $\dot{\varphi}c_0^{-1}$ vanishes as t goes infinity in $z_2(t)$. On the other hand, Ξ is bounded as previously shown, and $\tilde{\mathcal{K}}_b^{-1}$ is a strictly proper and stable transfer function. Thus the boundedness of $\tilde{\mathcal{K}}_b^{-1}\{\Xi^T\}$ can be concluded, which in turn results in converging $\tilde{\mathcal{K}}_b^{-1}\{\Xi^T\}\{\frac{\dot{\varphi}}{c_0}\}$ to zero. Therefore, as $\tilde{\mathcal{M}}\tilde{\mathcal{L}}\tilde{\mathcal{K}}_c^{-1}$ is a strictly proper and stable transfer function, the convergence of $z_2(t)$ to zero for sufficiently large t is obtained, which completes the prove and guarantees $\lim_{t\to\infty}e_o(t)=0$. □

5. Higher-order tracking

In this subsection, we extend the capability of the IE-MRAC mechanism. As one can see, this idea guarantees the convergence of the first-order derivative of the output error to zero for the LVC, as well as the original signal.

Theorem 2. *In the IE-MRAC of the LV, in addition to the output error (i.e., speed tracking error), its first-order derivative also tends to zero as t approaches infinity or*

$$\lim_{t\to\infty}\frac{\mathrm{d}^k e_o(t)}{\mathrm{d}t^k}=0$$

for $k=0,\ 1$.

Proof. By taking the first-order derivative of Eq. (7), and applying $s\Pi(s) + \lambda(s) = 1$ to the both sides, one can yield

$$\dot{e}_o(t) = \frac{1}{c_0^*}\tilde{\Pi}\tilde{\mathcal{M}}s^2\{\boldsymbol{\varphi}^T(t)\boldsymbol{\varpi}(t)\} + \frac{1}{c_0^*}\tilde{\lambda}s\{e_0(t)\}.$$

Since $\tilde{\mathcal{M}}s^2$ is proper and stable, $\frac{1}{c_0^*}\tilde{\mathcal{M}}s^2\{\boldsymbol{\varphi}^T(t)\boldsymbol{\varpi}(t)\}$ is bounded and also, $s\tilde{\lambda}$ is a strictly proper and stable filter. Thus, by following the same line as the approach of showing the convergence of the output error to zero, it can be shown that

$$\lim_{t\to\infty}\frac{\mathrm{d}e_o(t)}{\mathrm{d}t} = 0. \quad \square$$

By using a similar trend, it can be verified that for a reference model with the relative degree κ in the IE-MRAC, we have

$$\lim_{t\to\infty}\frac{\mathrm{d}e_o^{(q)}(t)}{\mathrm{d}^q t} = 0$$

for $q = 1, \ldots, \kappa - 1$.

Corollary 1. *If the first-order derivative of the reference signal is bounded $\dot{r}(t) \in L_\infty$, then IE-MRAC of LV has the following convergence property:*

$$\lim_{t\to\infty}\frac{\mathrm{d}^k e_o(t)}{\mathrm{d}t^k} = 0$$

for $k = 0,\ 1,\ 2$.

Proof. By taking the second-order derivative from the output error, the following equation is received

$$e_o^{(2)}(t) = \frac{1}{c_0^*}\tilde{\Pi}\tilde{\mathcal{M}}s^2\left\{s\{\boldsymbol{\varphi}^T(t)\boldsymbol{\varpi}(t)\}\right\} + \frac{1}{c_0^*}\tilde{\lambda}s\{\dot{e}_0(t)\}.$$

As it can be seen, if the boundedness of $s\{\boldsymbol{\varphi}^T(t)\boldsymbol{\varpi}(t)\}$ be ensured, by employing the results acquired so far, the convergence of $e_o^{(2)}(t)$ to zero can be concluded. Since $\boldsymbol{\varphi}$, $s\{\boldsymbol{\varphi}\}$ and $\boldsymbol{\varpi}$ are bounded, the boundedness of $s\{\boldsymbol{\varphi}^T(t)\boldsymbol{\varpi}(t)\}$ can be resulted by ensuring the boundedness of $s\{\boldsymbol{\varpi}\}$, that is

$$s\{\boldsymbol{\varpi}\} = \begin{bmatrix}\dot{r}(t) & s\{\varpi_1\} & \dot{v}(t) & s\{\varpi_2\}\end{bmatrix}$$

where $\dot{r}(t)$ is bounded by assumption and $\dot{v}(t)$ was previously proven to be bounded (see Eq. (26)). The $s\{\varpi_1\}$, $s\{\varpi_2\}$ are bounded because the bounded signals $u_t(t)$ and $v(t)$ are filtered through a proper and stable transfer function, respectively. Therefore,

$$\lim_{t\to\infty}\frac{\mathrm{d}^2 e_o(t)}{\mathrm{d}t^2} = 0$$

which completes the proof. $\square$

The Corollary 1 can be extended to the general case when the relative degree of the reference model is κ, resulting in the κ-th order tracking.

6. Modifications for robustness

In the control design subsection, it was assumed that the longitudinal model is linear and time-invariant, and the signals are measured precisely, which are the best possible situations that can occur. However, in the practical implementation, systems may vary with operating conditions such as gear shifting and road conditions in the longitudinal model [3]. Moreover, the collected data from measurement is mostly affected by noise. Here, a modification of the adaption law is proposed to ensure the robust performance of the presented control design.

In this manuscript, the longitudinal model is considered as a linear and slowly time-variant case, which is an approximation of a nonlinear dynamic around the operating condition. These assumptions, however, may be violated by nonlinearities in the system, tire characteristics, dynamic changes in vehicle mass, impact of road conditions, temperature effects on engine performance, nonlinearities in throttle response, external disturbances such as wind gusts, changes in wind direction, time delays. These situations can result in growing the controller parameters in an unbounded fashion. To avoid such drift and ensure the boundedness of parameters in the presence of uncertainties, the adaptive law Eq. (16) must be improved. A natural solution is to add a damping term to the update law, which is known as leakage [25]. The σ-modification is one of the leakage methods aiming to introduce a modification term into the standard adaptive law to prevent the parameters from drifting too far, guaranteeing stability even in the face of uncertainties, which is achieved by ensuring that the time derivative of the Lyapunov function employed to analyze the adaptive scheme, becomes negative within the space of parameter estimates when these parameters surpass specified bounds: [25]:

$$\dot{\boldsymbol{\vartheta}}(t) = -\rho\frac{e_i\boldsymbol{\Xi}(t)}{1 + \zeta\boldsymbol{\Xi}^T(t)\boldsymbol{\Xi}(t)} - \sigma\boldsymbol{\vartheta}(t) \tag{35}$$

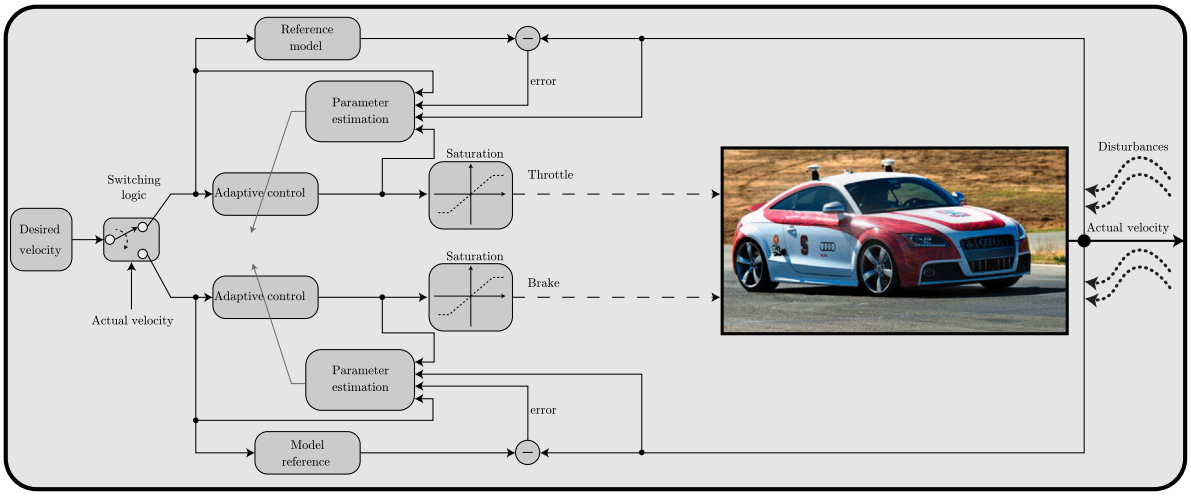

Fig. 2. The schematic of proposed adaptive control.

where σ is a positive constant. The modified adaption law Eq. (35) guarantees the boundedness of control parameters, but it has the drawback of having a nonzero error, even when all assumptions are perfectly assured [25]. Because the motivation for using the σ-modification is to guarantee the boundedness of controller parameters, it is rational to be inactive whenever the parameters are inside some predefined admissible bounds. Thus, a more sensible choice would be as follows

$$\dot{\vartheta}_i(t) = \begin{cases} -\boldsymbol{\Gamma}_{ii} \frac{e_i \Xi(t)}{1+\zeta \Xi^T(t)\Xi(t)} & \left|\vartheta_i(t)\right| < \delta_i \\ -\boldsymbol{\Gamma}_{ii} \frac{e_i \Xi(t)}{1+\zeta \Xi^T(t)\Xi(t)} - \sigma(\left|\vartheta_i(t)\right| \delta_i^{-1} - 1)\vartheta_i(t) & \delta_i \le \left|\vartheta_i(t)\right| \le 2\delta_i \\ -\boldsymbol{\Gamma}_{ii} \frac{e_i \Xi(t)}{1+\zeta \Xi^T(t)\Xi(t)} - \sigma \vartheta_i(t) & \left|\vartheta_i(t)\right| > 2\delta_i \end{cases}$$

which is known as switching σ-modification. The first adaptive law implies that if the parameters are within acceptable ranges, the original adaptive law is used to maintain convergence properties. In case of having unexpected large values, the term should be activated through second and third adaptive laws. The second adaptive law is used for smooth switching between the first and third, avoiding oscillations on the switching surface. Notice that δ_i is a constant that should satisfies $\delta_i > \left|\vartheta_i^*\right|$. The determination of δ_i is one of the main limitations of using such modifications that must be considered. Some methods exist to empirically determine the value of δ_i, which has been discussed in [27]. In this paper, the proposed method is applied to the vehicle several times without any robust modification, and the controller parameters are observed at various operating conditions. These observations lead to considering a bound on each parameter such that the parameter drifts from the admissible bounds are avoided. As a result, using such a method will ensure the boundedness of controller parameters.

7. Simulation results

Until now, the proposed controller has been designed for the throttle; however, to control the LV, the control of the braking system is needed. The behavior of the braking system is profoundly affected by some physical situations, including friction and temperature. The friction causes a nonlinear behavior in the braking system, while the temperature makes the performance time-variant. Our approach to controlling the braking system is the same as the throttle control, in which the brake level is related to the corresponding deceleration through a second-order linear system with slowly time-variant parameters. Using simplified relation (a cubic polynomial) for specific operating conditions has been experimentally validated in [3]. In this respect, we used a second-order model for the brake system, capturing more characteristics than a polynomial function and keeping the control design simple enough as a unified control structure is used for both the throttle and brake systems. Although the behavior of the braking system is considered a linear system, employing the modified IE-MRAC with the robust adaptive control law, as will be shown in this section, performs acceptably for controlling LV.

In this section, the proposed method is applied to the precise vehicle model software package known as CarSim [28]. The CarSim is an accurate vehicle simulator that provides precise, complete, and efficient techniques to predict the response of vehicles to the control inputs (e.g., throttle, brakes, steering, clutch) in a designable environment. The proposed adaptive control design schematic is illustrated in Fig. 2, and the software implementation is depicted in Fig. 3. Based on the development, the reference model for simulations should be in the form of a second-order system. In this respect, we have selected the following reference model:

$$\mathcal{M}(s) = \frac{1}{s^2 + 2s + 1} \tag{36}$$

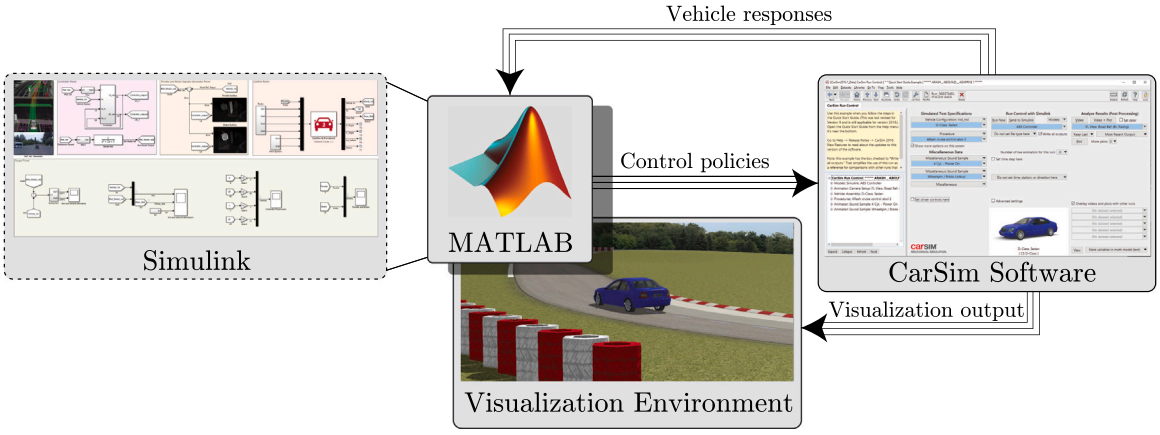

Fig. 3. The software implementation of the proposed adaptive control.

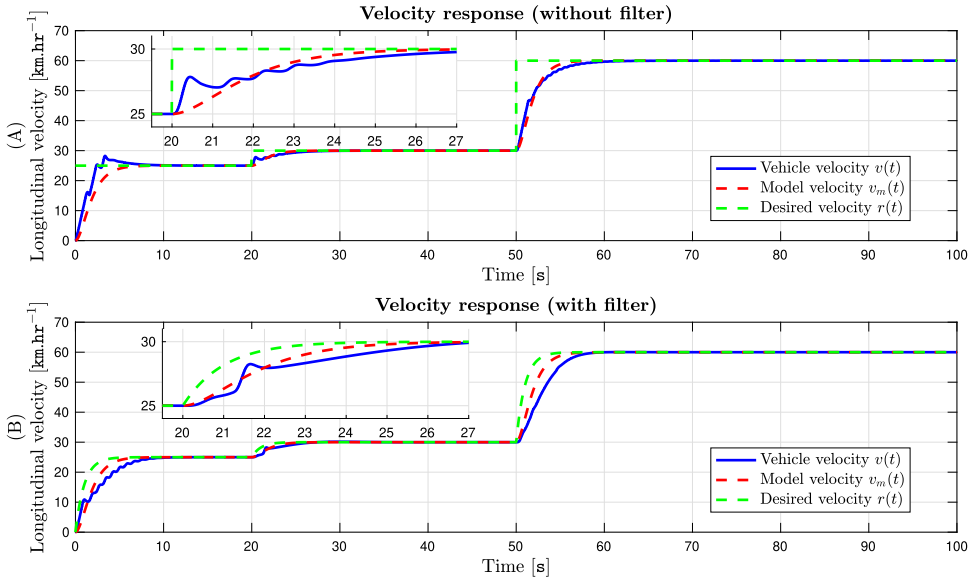

Fig. 4. (A) LVC on a straight path without filtering the reference signal. (B) LVC on a straight path with filtering of the reference signal.

which has the damping ratio of one, indicating a critically damped response. This can provide fast and smooth tracking of the reference signal. The filters $\phi(s)$ and $\mathcal{L}^{-1}(s)$ are considered as

$$\phi(s) = s + 1, \quad \mathcal{L}^{-1}(s) = \frac{1}{s^2 + 3s + 4}$$

where $\mathcal{L}^{-1}(s)$ is chosen so that $\tilde{\mathcal{M}}\tilde{\mathcal{L}}$ is proper. After conducting several experiments, we selected the parameters of the adaptive law to achieve a balance between rapid convergence and stability. The parameters were set as: $\Gamma = -10 \times I_3$ and $\zeta = 1$, ensuring relatively fast convergence while minimizing oscillatory behavior. In implementing the σ-modification algorithm, we set $\delta_i = 100$, a decision guided by observations of the controller parameters, which approximately range around 2. Finally, we used $\sigma = 0.1 \times \delta_i = 10$ for the leakage parameter.

First, a straight path is chosen, and the results are provided in Figs. 4–6(A). As can be seen, the actual velocity in Fig. 4(A) successfully tracks the reference velocity. The control parameters in Fig. 5(A) vary slowly, referring to the operating conditions, such as gear shifting, changes in reference velocity, and path situations. Frequent gear shifting and non-smooth throttle signal are observed in Fig. 5(A), and moreover, the second-order derivative of the output error is not converged to zero, as can be concluded from Fig. 6(A). Theorem 2 guarantees the first-order tracking that has been achieved (Fig. 6(A)). However, to ensure the second-order tracking and using the result of Corollary 1, the step reference function should be filtered to be smooth and have a bounded first-order derivative. In this manuscript, the following transfer function is used to filter the reference input

$$r_f(t) = \frac{1}{0.001s^2 + 1s + 1}. \tag{37}$$

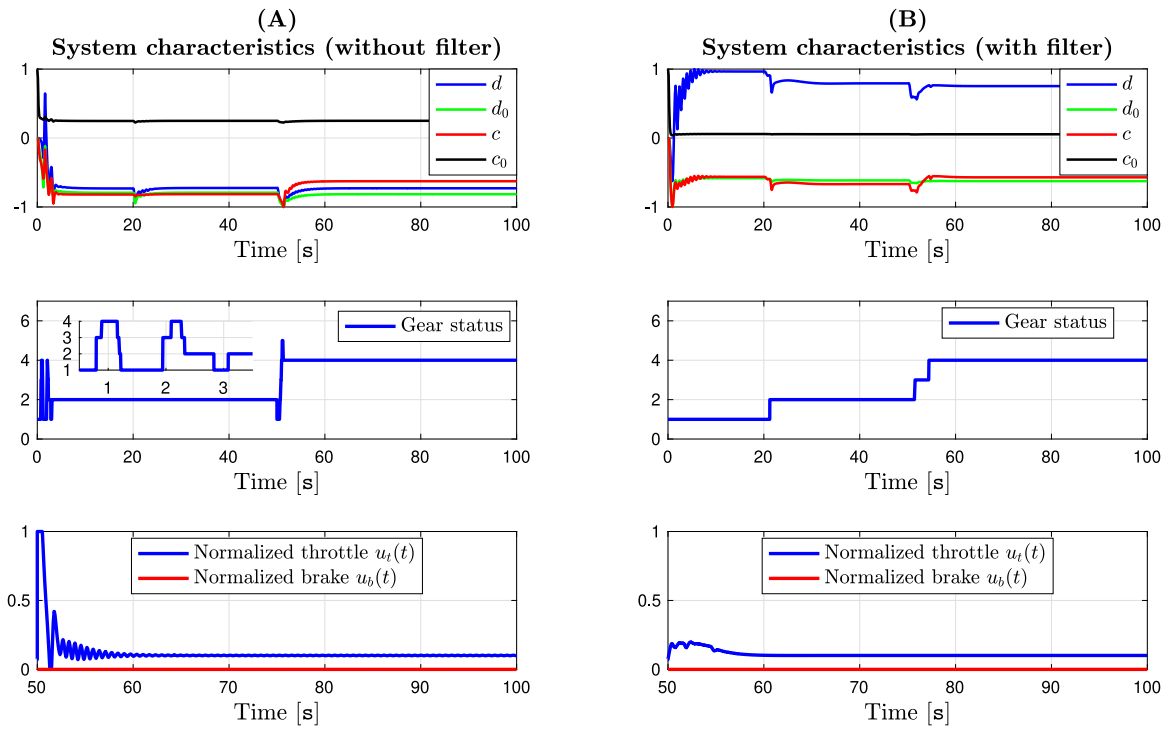

Fig. 5. (A) Control parameters, gear status, and normalized throttle/brake signals without filtering the reference signal. (B) Control parameters, gear status, and normalized throttle and brake signals with filtering of the reference signal.

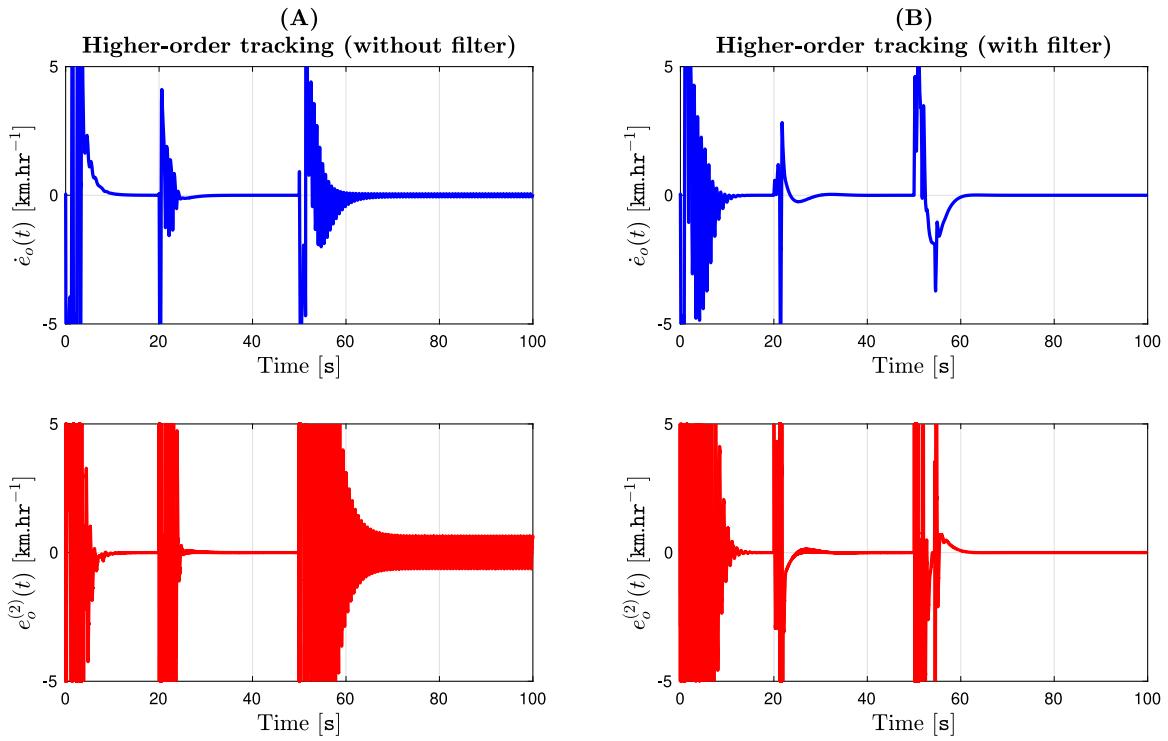

Fig. 6. (A) First and second order derivatives of the output error without filtering the reference signal. (B) First and second-order derivatives of the output error with filtering of the reference signal.

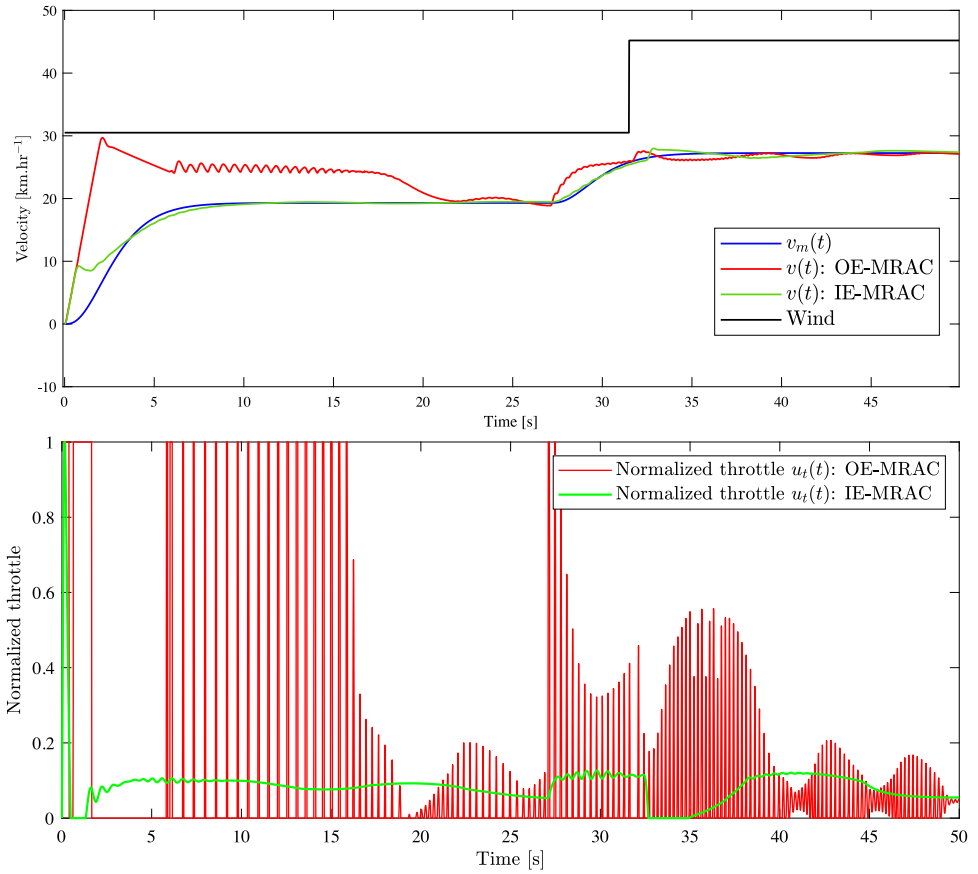

Fig. 7. Performance comparison of the IE-MRAC and OE-MRAC controllers.

The selection of the filter provides very fast-tracking of the step command (desired velocity) and ensures higher-order tracking. The simulation results are provided in Figs. 4–6(B). As can be observed, second-order tracking is achieved, frequent gear-shifting is avoided, and the throttle signal is almost smooth. The convergence of the second-order derivative of the output error to zero implies that the abrupt variations in the system are avoided. Consequently, the acceleration is decreased and kept limited. Such improvements in response lead to passenger comfort and reduce aging and maintenance costs.

Remark 2. Since the objective of the MRAC is to follow the output of a reference model, by adjusting the characteristics of the reference model, including settling time, rise time, and overshoot, the comfort of passengers can be captured.

In the next simulation, we aim to compare the performance of the IE-MRAC and OE-MRAC for controlling LV. Directly designing OE-MRAC with the structure outlined in the preliminaries is not feasible, as the reference model does not satisfy the SPR condition. To address this issue, we employed an augmented error scheme as presented in [18,23]. The simulation results, depicted in Fig. 7, illustrate the performance in terms of used throttle settings and actual velocity. The results clearly indicate the limitations of OE-MRAC for the ACC system; it fails to achieve the tracking objective, and the throttle input is impractical and undesired. In contrast, IE-MRAC successfully controls the LV with reasonable throttle settings. One potential source of error when using OE-MRAC is the inability to perform acceptably in the presence of input saturation, leading to erroneous identification, as stated in the following remark. In the beginning, both controllers experience saturation. Unlike OE-MRAC, the input-error-based strategy effectively manages such limitations on the throttle.

Remark 3. One of the main differences between the output and input MRAC is when the input to the system saturates. The error derived in OE-MRAC depends on the control signals $u(t)$ being the same as the calculated one $u(t) = \boldsymbol{\vartheta}^T(t)\boldsymbol{\varpi}(t)$; thus, identification in the presence of saturation will be inaccurate (see [18,29]). However, such difficulty is absent in the IE-MRAC since the derived error equation Eq. (39) that uses Eq. (14) does not rely on any specified value of $u(t)$. Therefore, the proposed technique can deal with saturation on both throttle and brake input signals, and no modification of the adaptive law is needed in this case.

In the next step, the simulation test is carried out through unfavorable and more realistic path conditions, including road curves, banking, and elevation, and the aerodynamic effects are applied by inserting wind in the opposite direction of the LV. The simulation

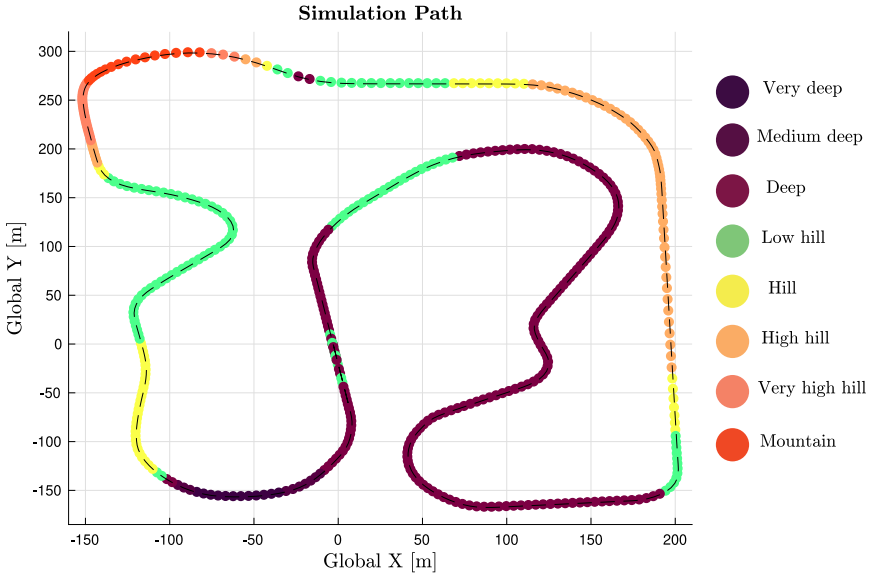

Fig. 8. The designed path for simulation.

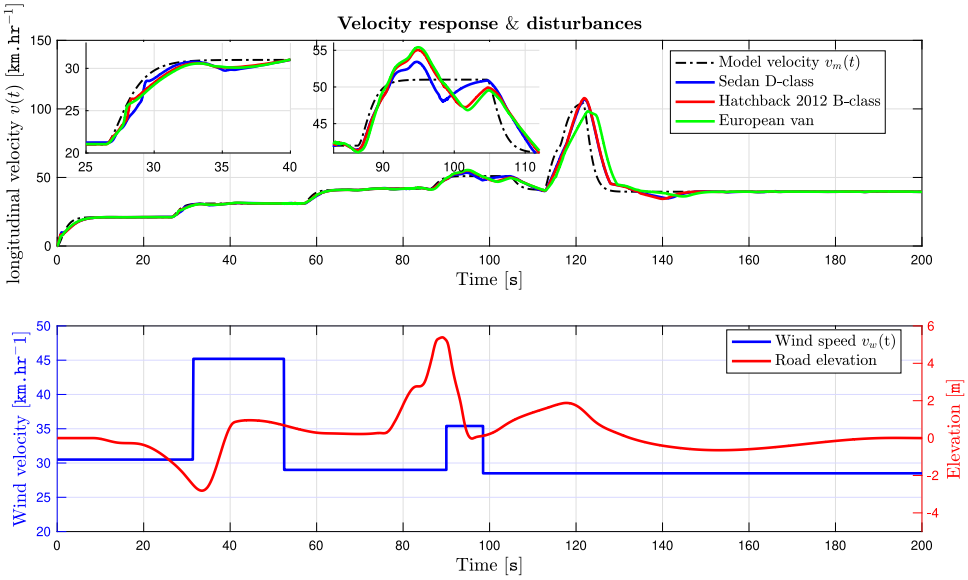

Fig. 9. The comparison between the velocity responses of three different vehicle classes in CarSim, wind velocity in the opposite direction of LV, and road elevation.

path is illustrated in Fig. 8. The proposed robust IE-MRAC is applied to the three different classes of vehicles in CarSim, and the results are depicted in Figs. 9,10. Fig. 9 reveals that the three types of vehicles have successfully tracked the reference command in adverse path conditions. As can be seen from Fig. 9, the road elevation changes continuously, and the aerodynamic force is permanently present. Therefore, a high-performance control design is needed to handle such disturbances. The modified IE-MRAC has performed well, and as can be observed from Fig. 10, the control signals were obtained so that the adaption to the change of conditions has occurred. The results depict that vehicles' responses are different from each other. However, they have followed the desired velocity acceptably. The reason is apparent because these vehicles have different technical specifications, including mass, dimensions, cylinders, maximum power, and maximum torque; their dynamics are different, which leads to different control parameters and, as a result, different responses. However, in all cases, the control signals were received such that the reference velocities were tracked. As a result, the proposed approach can successfully handle various road conditions and vehicle dynamics, which implies the method's applicability.

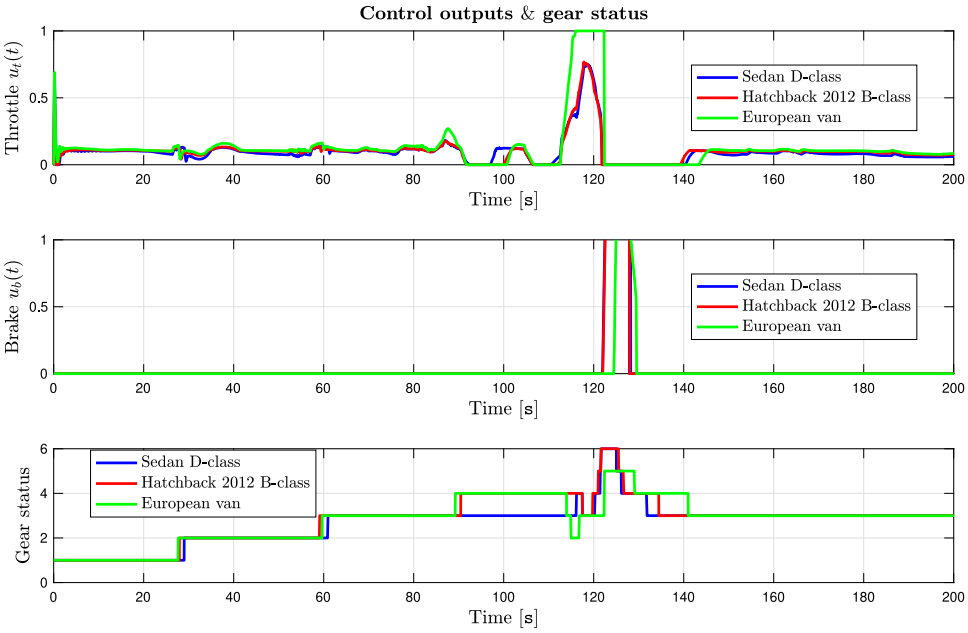

Fig. 10. The comparison between the throttle/brake signals and gear status of three different vehicle classes CarSim.

Remark 4. Since a generic model of cars is used in designing the adaptive controller, it can be applied to a vast majority of vehicles without knowing the exact vehicle powertrain and brake system.

Remark 5. The proposed method is not restricted to step tracking; a ramp or combination of ramp and step commands can be tracked. However, the reference model and controller structure differ in this case. For instance, the following reference model can ensure the track of combined ramp and step reference velocities:

$$\mathcal{M}(s) = \frac{bs + a}{s^3 + cs^2 + bs + a} \tag{38}$$

where a, b, and c are constants that determine the characteristics of the responses. Notice that the chosen model Eq. (38) satisfies the assumptions $\mathcal{A}$-IE2 and $\mathcal{A}$-IE3, thus the IE-MRAC can be employed, and the HOT properties are still held.

8. Conclusion

In this paper, the IE-MRAC was employed to control the LV of autonomous vehicles. It was shown that the IE-MRAC performs better than the classical OE-MRAC owing to handling saturation on input signals, having a linear regression error equation, and performing more robustly. Besides the analysis of IE-MRAC properties, a novel stability proof was presented and given within a theorem. The presence of modeling error, time-varying parameters, nonlinear behavior, disturbances, and noisy measurements led us to modify the IE-MRAC with a robust adaptive control law to guarantee the boundedness of the controller parameters in the presence of uncertainties. The unknown approximation of the longitudinal model was forced to follow a predefined reference model by generating bounded throttle/brake control signals. Although the results were satisfactory, by stating the higher-order tracking property and proving it for the longitudinal velocity control, we showed that second-order tracking could be achieved via smoothing the reference signal. Moreover, it enhanced vehicle responses, such as smoothing the throttle/brake signals and avoiding frequent gear shifting. Such improvements in response lead to passenger comfort because the variation in acceleration is decreased and kept limited. The applicability of the presented approach was validated by the CarSim simulator by considering realistic path conditions such as road curves, banking, elevation, and the presence of aerodynamic effects.

CRediT authorship contribution statement

Abolfazl Simorgh: Writing, Mathematical derivations, Formal analysis, Methodology, Resources, Validation. **Abolhassan Razminia:** Original idea, Investigation, Writing – review & editing. **Arash Marashian:** Simulations, Visualization, Programming, Validation, Formal analysis.

Declaration of competing interest

The authors declare that they have no known competing financial interests or personal relationships that could have appeared to influence the work reported in this paper.

Funding acknowledgment

The authors received no financial support for the research, authorship, and/or publication of this article.

Code availability

The Simulink files used in this study can be accessed using Link.

Appendix A. Effect of the initial condition on the stability proof

In presenting the proposed IE-MRAC for ACC, we ignored the effects of the initial condition. However, given the nonlinearity of the overall system, it becomes imperative to demonstrate that neglecting this term does not impact the stability analysis. To show that, we will use a similar approach presented in [23]. We show boundedness of $\boldsymbol{\varphi}$ and also $\dot{\boldsymbol{\varphi}} \in L_2$ which are central to prove stability is not affected by the initial condition. The remaining parts of stability proof are related to arguments about the unboundedness of signals and, therefore, unchanged by $\varepsilon(t)$. The original input error equation is given in the following:

$$e_i = \boldsymbol{\varphi}^T(t)\boldsymbol{\Xi}(t) - \varepsilon(t). \tag{39}$$

The update law without considering $\varepsilon(t)$ is:

$$\dot{\boldsymbol{\varphi}}(t) = -\frac{\boldsymbol{\Xi}(t)\boldsymbol{\Xi}(t)^T}{1+\zeta\boldsymbol{\Xi}^T(t)\boldsymbol{\Xi}(t)}\boldsymbol{\varphi}(t). \tag{40}$$

By selecting the following Lyapunov function:

$$V(\varphi(t)) = 0.5\cdot\varphi^T(t)\varphi(t) \tag{41}$$

we obtain the time derivative evaluated along the trajectories of Eq. (40) as

$$\dot{V}(\varphi(t)) = \frac{e_i^2(t)}{1+\zeta\boldsymbol{\Xi}^T(t)\boldsymbol{\Xi}(t)} \le 0 \tag{42}$$

implying that $\boldsymbol{\varphi}(t)$ is uniformly bounded. In addition, as $-\int_{t_0}^{\infty}\dot{V}\,\mathrm{d}t = -V(\infty) + -V(t_0) \le \infty$, we have $e_i(t)\cdot(1+\zeta\boldsymbol{\Xi}^T(t)\boldsymbol{\Xi}(t))^{-0.5} \in L_\infty$. From Eq. (40), we conclude, $\dot{\boldsymbol{\varphi}} \in L_\infty \cap L_2$. Now let us consider the original error equation with the effects of initial condition. The update law with projection is obtained as:

$$\dot{\boldsymbol{\varphi}}(t) = \frac{\boldsymbol{\Xi}(t)\boldsymbol{\Xi}(t)^T}{1+\zeta\boldsymbol{\Xi}^T(t)\boldsymbol{\Xi}(t)}\boldsymbol{\varphi}(t) - \frac{\boldsymbol{\Xi}(t)\epsilon(t)}{1+\zeta\boldsymbol{\Xi}^T(t)\boldsymbol{\Xi}(t)} \tag{43}$$

$\epsilon(t)$ can be considered the output of a system, represented by:

$$\dot{\mathbf{p}} = M\mathbf{p}, \quad \epsilon(t) = \mathbf{m}^T\mathbf{p} \tag{44}$$

where M is a stable matrix and the pair $(\mathbf{m}^T, M)$ is detectable. We select the following Lyapunov function

$$V(\varphi(t), \mathbf{p}) = 0.5\cdot\varphi^T(t)\varphi(t) + 0.25\cdot\mathbf{p}^T P\mathbf{p} \tag{45}$$

where

$$M^T P + PM = -\mathbf{m}\mathbf{m}^T - Q; \quad P = P^T \succ 0,\ Q \succ 0. \tag{46}$$

By taking derivative along the trajectories Eqs. ((43), (44)), the following equation is received:

$$\begin{aligned}\dot{V} &\le -\frac{(\boldsymbol{\varphi}^T(t)\boldsymbol{\Xi})^2}{1+\zeta\boldsymbol{\Xi}^T(t)\boldsymbol{\Xi}(t)} - \frac{(\boldsymbol{\varphi}^T(t)\boldsymbol{\Xi})\epsilon(t)}{1+\zeta\boldsymbol{\Xi}^T(t)\boldsymbol{\Xi}(t)} - \frac{\epsilon^2}{4} \\ &= \left(\frac{\boldsymbol{\varphi}^T(t)\boldsymbol{\Xi} + 0.5\epsilon(t)}{\sqrt{1+\zeta\boldsymbol{\Xi}^T(t)\boldsymbol{\Xi}(t)}}\right)^2 - \frac{\zeta\boldsymbol{\Xi}^T(t)\boldsymbol{\Xi}(t)\epsilon^2(t)}{4(1+\zeta\boldsymbol{\Xi}^T(t)\boldsymbol{\Xi}(t))}.\end{aligned} \tag{47}$$

It can be concluded that $\varphi \in L_\infty$ and $\dot{\varphi} \in L_2$, and thus, the results are identical to the case that the term $\epsilon(t)$ was neglected.

Appendix B. Supplementary data

Supplementary material related to this article can be found online at https://doi.org/10.1016/j.jfranklin.2024.106700.

References

[1] R. Rajamani, Vehicle Dynamics and Control, Springer Science & Business Media, 2011.
[2] S. Moon, K. Yi, Human driving data-based design of a vehicle adaptive cruise control algorithm, Veh. Syst. Dyn. 46 (8) (2008) 661–690.
[3] J.E.A. Dias, G.A.S. Pereira, R.M. Palhares, Longitudinal model identification and velocity control of an autonomous car, IEEE Trans. Intell. Transp. Syst. 16 (2) (2015) 776–786.
[4] S. Moon, I. Moon, K. Yi, Design, tuning, and evaluation of a full-range adaptive cruise control system with collision avoidance, Control Eng. Pract. 17 (4) (2009) 442–455.
[5] L. Vite, L. Juárez, M.A. Gomez, S. Mondié, Dynamic predictor-based adaptive cruise control, J. Franklin Inst. B 359 (12) (2022) 6123–6141.
[6] A. Tapani, Vehicle trajectory effects of adaptive cruise control, J. Intell. Transp. Syst. 16 (1) (2012) 36–44.
[7] M. Brown, J. Funke, S. Erlien, J.C. Gerdes, Safe driving envelopes for path tracking in autonomous vehicles, Control Eng. Pract. 61 (2017) 307–316.
[8] H. Kim, D. Kim, I. Shu, K. Yi, Time-varying parameter adaptive vehicle speed control, IEEE Trans. Veh. Technol. 65 (2) (2016) 581–588.
[9] Y. Ying, T. Mei, Y. Song, Y. Liu, A sliding mode control approach to longitudinal control of vehicles in a platoon, in: 2014 IEEE International Conference on Mechatronics and Automation, 2014, pp. 1509–1514.
[10] Z. Liang, J. Zhao, B. Liu, Y. Wang, Z. Ding, Velocity-based path following control for autonomous vehicles to avoid exceeding road friction limits using sliding mode method, IEEE Trans. Intell. Transp. Syst. 23 (3) (2020) 1947–1958.
[11] D. Theodosis, I. Karafyllis, M. Papageorgiou, Cruise controllers for lane-free ring-roads based on control Lyapunov functions, J. Franklin Inst. B 360 (9) (2023) 6131–6161.
[12] Y. Chen, J. Wang, Adaptive vehicle speed control with input injections for longitudinal motion independent road frictional condition estimation, IEEE Trans. Veh. Technol. 60 (3) (2011) 839–848.
[13] J.E. Naranjo, C. Gonzalez, R. Garcia, T. de Pedro, ACC+Stop&Go maneuvers with throttle and brake fuzzy control, IEEE Trans. Intell. Transp. Syst. 7 (2) (2006) 213–225.
[14] J. Zhan, T. Zhang, J. Shi, X. Guan, Z. Nan, N. Zheng, A dual closed-loop longitudinal speed controller using smooth feedforward and fuzzy logic for autonomous driving vehicles, in: 2021 IEEE International Intelligent Transportation Systems Conference, ITSC, IEEE, 2021, pp. 545–552.
[15] S. Chen, H. Chen, MPC-based path tracking with PID speed control for autonomous vehicles, in: IOP Conference Series: Materials Science and Engineering, vol. 892, (no. 1) IOP Publishing, 2020, p. 012034.
[16] M. Zhu, H. Chen, G. Xiong, A model predictive speed tracking control approach for autonomous ground vehicles, Mech. Syst. Signal Process. 87 (2017) 138–152, Signal Processing and Control challenges for Smart Vehicles.
[17] M. Jalali, E. Hashemi, A. Khajepour, S.-k. Chen, B. Litkouhi, Model predictive control of vehicle roll-over with experimental verification, Control Eng. Pract. 77 (2018) 95–108.
[18] S. Sastry, M. Bodson, Adaptive Control: Stability, Convergence and Robustness, Courier Corporation, 2011.
[19] K.S. Narendra, A.M. Annaswamy, Stable Adaptive Systems, Courier Corporation, 2012.
[20] H. Bagherpoor, F.R. Salmasi, Robust model reference adaptive output feedback tracking for uncertain linear systems with actuator fault based on reinforced dead-zone modification, ISA Trans. 57 (2015) 51–56.
[21] N. Barabanov, R. Ortega, On the need of projections in input-error model reference adaptive control, Internat. J. Adapt. Control Signal Process. 32 (3) (2018) 403–411.
[22] M. Bodson, Tuning, multitone instabilities, and intrinsic differences in robustness of adaptive control systems, IEEE Trans. Automat. Control 39 (4) (1994) 864–870.
[23] K.S. Narendra, A.M. Annaswamy, R.P. Singh, A general approach to the stability analysis of adaptive systems, Internat. J. Control 41 (1) (1985) 193–216.
[24] K. Narendra, Y.-H. Lin, L. Valavani, Stable adaptive controller design, part II: Proof of stability, IEEE Trans. Automat. Control 25 (3) (1980) 440–448.
[25] P.A. Ioannou, J. Sun, Robust Adaptive Control, Courier Corporation, 2012.
[26] G. Tao, G. Song, Higher order tracking properties of model reference adaptive control systems, IEEE Trans. Automat. Control 63 (11) (2018) 3912–3918.
[27] Y. Yildiz, A.M. Annaswamy, D. Yanakiev, I. Kolmanovsky, Spark-ignition-engine idle speed control: An adaptive control approach, IEEE Trans. Control Syst. Technol. 19 (5) (2011) 990–1002.
[28] Mechanical Simulation-CarSim, https://www.carsim.com/products/carsim/index.php.
[29] G. Goodwin, D. Mayne, A parameter estimation perspective of continuous time model reference adaptive control, Automatica 23 (1) (1987) 57–70.